

Geophysical Research Letters®



RESEARCH LETTER

10.1029/2024GL109569

A Novel Connectivity Metric of Identified Multi-Cluster Fracture Networks in Permeable Formations

Weiwei Zhu^{1,2,3} , Xupeng He⁴, Tadeusz Wiktor Patzek⁵, Zhiqiang Chen⁶, Hussein Hoteit⁵ ,
Derek Elsworth⁷, Shengwen Qi^{1,2} , and Moran Wang³ 

¹Key Laboratory of Shale Gas and Geoen지니어ing, Institute of Geology and Geophysics, Chinese Academy of Sciences, Beijing, China, ²College of Earth and Planetary Sciences, University of Chinese Academy of Sciences, Beijing, China, ³Department of Engineering Mechanics, Tsinghua University, Beijing, China, ⁴EXPEC Advanced Research Center, Saudi Aramco, Dhahran, Saudi Arabia, ⁵Ali I. Al-Naimi Petroleum Engineering Research Center (ANPERC), King Abdullah University of Science and Technology, Thuwal, Saudi Arabia, ⁶Petroleum Exploration and Production Research Institute, SINOPEC, Beijing, China, ⁷Department of Energy and Mineral Engineering, EMS Energy Institute and G3 Center, Pennsylvania State University, University Park, PA, USA

Key Points:

- Fracture sealing significantly impacts overall connectivity, with 5% of sealed fractures reducing it by about 20%
- Altering the central cluster insignificantly affects connectivity but significantly influences production
- Natural fractures enhance connectivity by linking clusters, with heterogeneity and anisotropy playing a pivotal role

Supporting Information:

Supporting Information may be found in the online version of this article.

Correspondence to:

M. Wang and S. Qi,
mrwang@tsinghua.edu.cn;
qishengwen@mail.iggcas.ac.cn

Citation:

Zhu, W., He, X., Patzek, T. W., Chen, Z., Hoteit, H., Elsworth, D., et al. (2024). A novel connectivity metric of identified multi-cluster fracture networks in permeable formations. *Geophysical Research Letters*, 51, e2024GL109569. <https://doi.org/10.1029/2024GL109569>

Received 7 APR 2024
Accepted 11 JUL 2024

Abstract Complex natural fracture networks typically consist of multiple clusters, whose connectivity is rarely quantified. Therefore, for each identified fracture network, we propose a connectivity metric that accounts for individual fracture clusters and their interactions. This metric evaluates contributions from all fracture clusters, considering their relative sizes and interactions among the isolated clusters, which in turn depend on the hydraulic conductance of the interconnecting rock matrix. Furthermore, we investigate how the system connectivity depends on fracture sealing, alterations of central clusters, and cluster linkage. Fracture sealing strongly impacts overall fracture connectivity, with 5 percent of sealed fractures reducing connectivity by 20 percent. The connectivity reduction is small when transitioning the central cluster from the largest to the smallest one. However, the largest cluster significantly contributes to overall connectivity, while the smallest one contributes minimally. Natural fracture networks increase connectivity by linking more clusters, with heterogeneity and anisotropy playing pivotal roles.

Plain Language Summary Natural fractures are typical multi-cluster systems found in many places, not just in crustal rocks but also in construction materials, human bones, and other areas. Multi-cluster systems are even more widespread, including in biological systems and materials science. In crustal rocks, natural fractures are crucial for assessing rock stability and flow processes because they control the mechanical and hydrological properties of the rocks. Thus, fractures are important in many engineering fields, such as oil and gas production and underground hydrogen or CO₂ storage. The connectivity of these multi-cluster systems is essential as it directly impacts their mechanical and hydrological properties. Here, we propose a new metric to measure the connectivity of complex fracture networks. This method explains how individual fracture clusters contribute and interact based on their sizes and hydraulic conductance. Applying this to outcrop fracture maps shows significant changes in network connectivity due to factors like fracture sealing, changes in central clusters, and cluster linkage. This method can also be applied to 3D fracture systems and other multi-cluster systems. These findings improve our understanding of how fractured formations evolve and how fluids flow through them, offering practical insights for better engineering practices.

1. Introduction

Fractures are ubiquitous in crustal rocks owing to the harsh environment in the deep subsurface and rock brittleness. Fractures are the planes of rock failure, significantly influence rock stability, and are pivotal factors in predicting geohazards (Blum et al., 2010; Qi et al., 2004; F. Renard et al., 2019). In addition, fractures usually provide a highly permeable pathways for fluid flow in the subsurface; therefore, they are crucial in oil and gas exploration and production, subsurface hydrogen storage, geological CO₂ sequestration, and nuclear waste disposal (Bond et al., 2013; Galloway et al., 2018; Orellana et al., 2019; Zoback & Smit, 2023).

Connectivity is the key characteristic of fracture networks, intricately tied to their effective hydraulic diffusivity. Extensive research has been undertaken in this realm (Alghalandis et al., 2015; Bour & Davy, 1997, 1998; Berkowitz et al., 2000; N. E. Odling, 1997; P. Renard & Allard, 2013; Xu et al., 2006; Ye et al., 2021; Zhu et al., 2021). However, key studies focus predominantly on connected fractures, especially on the largest cluster of

© 2024. The Author(s).

This is an open access article under the terms of the [Creative Commons Attribution License](https://creativecommons.org/licenses/by/4.0/), which permits use, distribution and reproduction in any medium, provided the original work is properly cited.

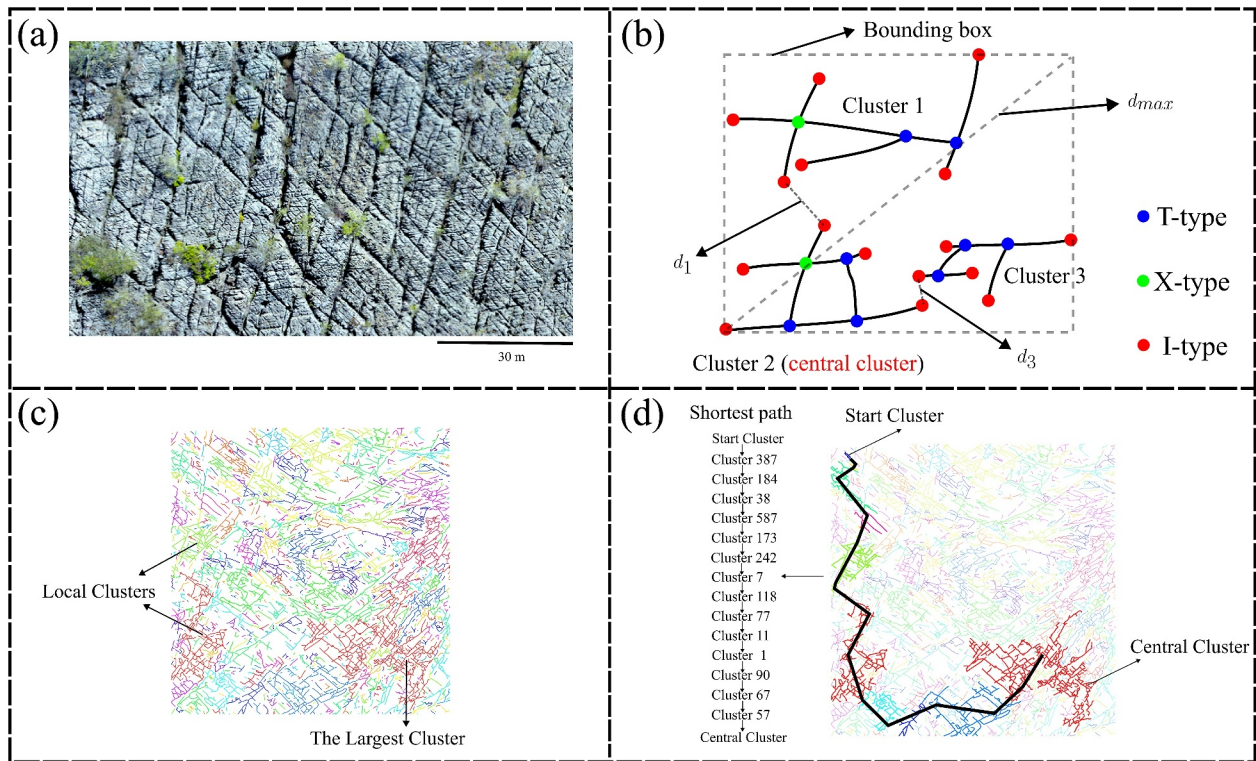


Figure 1. (a) Brejões Outcrop, Irecê Basin, Brazil (Prabhakaran et al., 2019). (b) A sketch map of a simple fracture network composed of three clusters. Different distances used in Equation 1 are denoted. T-type, X-type, and I-type nodes are marked in different colors. (c) Outcrop map (Map 3) of Hornelen basin, western Norway (N. E. Odling, 1997). Individual clusters have different colors. (d) The shortest distance between the start cluster and the central cluster. The distance is determined by traversing multiple intermediate clusters along the shortest path, ensuring the minimum distance in the permeable matrix.

fractures. Percolation theory (Allard & Group, 1993; Bour & Davy, 1997, 1998; Renshaw et al., 2017; Robinson, 1983), for instance, delves into the formation of the spanning cluster and the scaling behavior at the percolation threshold. The contributions of local clusters are rarely considered. While this simplification holds in cases of zero permeability of rock matrix, real rock formations invariably have matrices with non-zero permeabilities. Local fracture clusters with high permeability can reduce the flow path of fluid in a low-permeable matrix, thereby enhancing the overall connectivity of fractured media (Matthäi & Belayneh, 2004). Several methods, like the connectivity field, geological entropy, and the ternary diagram and its extension (Alghalandis et al., 2015; C. C. Barton et al., 1989; Sanderson & Nixon, 2015; Ye et al., 2021) are applicable for both single and multiple clusters. These methods usually focus on the topological structures and largely ignore the impacts of overall hydraulic conductance. Therefore, these methods are unsuitable to treat complex fracture networks composed of multiple clusters.

Natural fracture networks are always composed of multiple clusters, a phenomenon commonly observed in outcrop maps, see Figures 1a–1c. Even within a large cluster, fracture sealing due to compressive loads or crystal growth can lead to aperture reduction and division of a single cluster into multiple clusters with intricate sealing patterns (Im et al., 2018; Ukar & Laubach, 2016). Hence, quantifying the connectivity of systems comprising multiple clusters is crucial and holds significance beyond the realm of fracture networks, as multi-cluster systems exist in many scientific fields, such as materials science and biology.

To account for individual fracture clusters and their interactions, we proposed a new connectivity metric C_f (Section 2) and implement the metric to analyze natural fracture networks interpreted from real outcrop maps considering different conditions, including the impact of fracture sealing, alteration of central clusters, and cluster linkage. The results demonstrate connectivity variations and explain real-world phenomena, which has brought essential insights for us to understand subsurface fracture networks and have great potential for further analysis.

2. Materials and Methods

To account for individual fractures and their interactions, a straightforward yet powerful metric, C_i , is introduced for assessing the connectivity of natural fracture networks made up of multiple clusters. In this work, we implement the proposed metric on natural outcrop maps; therefore, the metric here is suitable for 2D fracture systems. However, it can be conveniently extended to 3D fracture systems, as demonstrated in the Discussion section.

$$C_i = \underbrace{\sum_{i=0}^n \left(\frac{k_m \mu_w}{k_f \mu} \right) \left(1 - \frac{d_i}{d_{\max}} \right)}_{\text{Interaction term}} \times \underbrace{\left(\frac{l_i}{l_{\text{total}}} \right)}_{\text{Individual term}} C_i \quad (1)$$

here n is the number of fracture clusters; k_m and k_f are the matrix and fracture permeabilities, respectively; μ and μ_w are the fluid and water viscosity, respectively; d_i represents the shortest distance in the matrix from cluster i to the central cluster; d_{\max} is the diagonal length of the bounding box that encloses all fractures in the considered fracture system; l_i denotes the total length of fractures in cluster i ; l_{total} is the total length of all fractures in the system; and C_i is the connectivity metric of cluster i . The parameters k_f , μ_w , and d_{\max} normalize the respective variables.

The newly defined metric focuses on two main aspects of connectivity. The individual terms in Equation 1 pertain to the connectivity of each cluster weighted by its relative size. The interaction terms account for the hydraulic conductance of the matrix between the central cluster and cluster i , $i = 1, 2, \dots, n$. The central cluster can be either the largest cluster or any other cluster, and the choice of the central cluster is one of the key factors discussed below.

In individual terms, C_i can represent any connectivity metric for cluster i . In this study, we adopt the average number of links for each branch as the metric of connectivity (Sanderson & Nixon, 2015). This choice is sufficient, because variable fracture apertures are excluded in the subsequent analysis of the fracture networks. Outcrop maps have experienced severe weathering and stress release during upward movement, which significantly changes fracture apertures. Therefore, aperture information from an outcrop map is generally unreliable. However, various apertures can also be incorporated with more complex connectivity metrics, such as global efficiency (Zhu et al., 2021).

$$C_i = \frac{3 \times N_T + 4 \times N_X}{N_B}, \quad (2)$$

where N_T , N_X , and N_B refer to the numbers of T -type, X -type nodes and branches. N_B is calculated with $1/2(N_I + 3N_T + 4N_X)$ and N_I is the number of I -type nodes. The respective node types are illustrated in Figure 1b. C_i is a dimensionless number between 0 and 2.0, with a larger value indicating better connectivity.

The key procedure to obtain the individual term is to find the T , X , and I -type nodes in the natural fracture outcrop, which is done by a novel pixel-based fracture detection algorithm (Zhu, He, Santoso, et al., 2022). Intersection nodes in the outcrop map are identified and classified into different node types based on the number of branches. The I -type nodes have only one branch, T -type nodes have three branches, and X -type nodes have four or more branches. Intersection nodes with more than four branches have a low probability of occurrence and constitute a tiny proportion of the outcrop map. Therefore, we have omitted them. If aperture variations of fractures are included, global efficiency can be used as the connectivity metric for individual clusters (Zhu et al., 2021).

In interaction terms, the flow between different clusters follows Darcy's law (Equation 2), and the term refers to the normalized hydraulic conductance of the matrix within them.

$$Q = \frac{k_m A}{\mu \Delta L} \Delta p \quad (3)$$

In comparing conductance with the interaction term, ΔL is replaced by d_i ; A represents the seepage area, which is related to the size of the cluster. Since we have accounted for the size effect in the individual term, the seepage

area is standardized to one for all cases considered in this work. For specific engineering applications, the actual permeability and viscosity can be used, while in this work, the coefficients regarding relative permeability and viscosity are also standardized to 1. The metric proposed in this work is dimensionless, as shown in Equation 1; therefore, it can be applied to any scale of fracture networks. However, the scale of fracture networks cannot be extremely small, where insufficient micropores exist to satisfy the representative elementary volume (REV) required for the implementation of Darcy's law.

The key procedure to obtain the interaction term is to calculate the shortest distance between two clusters. Directly considering the distance between a local cluster and the central cluster may not be suitable, as fluid in a distant local cluster can be indirectly connected to the central cluster through multiple intermediate clusters. Therefore, it is essential to determine the shortest distance in the matrix through these intermediate clusters (as shown in Figure 1d). To achieve this, the fracture system is transformed into a graph system. Each cluster is treated as a node, and up to 15 closest neighboring clusters are identified and linked to the cluster. The neighboring nodes are connected with links, where the length of the link represents the shortest distance between two node clusters. Selecting a sufficient number of neighboring clusters is critical to ensure that the fracture system forms a connected graph. However, an excessively large number can significantly increase computational complexity. Through trial and error, 15 is identified as an acceptable and sufficient value. Subsequently, the Dijkstra algorithm (Cormen et al., 2022) is applied to find the shortest paths between any arbitrary cluster and the central cluster. When considering two neighboring clusters i and j , the shortest distance between them is determined by finding the shortest distance between all pairs of line segments in the i th fracture cluster and the j th cluster. This problem is further decomposed into calculating the shortest distance between two line segments, which can be broken down into the shortest distance between the end nodes and the line segment.

The new metric is implemented to analyze natural fracture networks automatically interpreted from various outcrop maps from different published works (80 in total) with a novel fracture detection algorithm, which are spread across different parts of the world and vary in scale from millimeters to kilometers (C. C. Barton, 1995; Bertrand et al., 2015; Becker et al., 2018; Bisdorn, n.d.; Duffy et al., 2017; Gillespie et al., 1993; Healy et al., 2017; Holland et al., 2009; Jafari, 2011; N. E. Odling, 1997; N. Odling et al., 1999; Prabhakaran et al., 2021; Segall & Pollard, 1983; Thiele et al., 2017; Watkins et al., 2015; Wyller, 2019).

With the newly defined connectivity metric, we can quantify the connectivity of the entire fracture network and investigate the connectivity variations under different conditions, including the impact of fracture sealing, alteration of central clusters, and cluster linkage. These three conditions are commonly observed and essential for engineering practice. Fracture sealing occurs naturally, but its quantitative impact on the connectivity of complicated fracture networks is rarely discussed. The central cluster can be considered a distinct linkage zone for artificial instruments and natural fracture networks. For example, when drilling a vertical well, it may encounter a natural fracture cluster, which can be regarded as the central cluster. Different well positions lead to different central clusters, and, in turn, they affect the connectivity of the whole field and the final production. In fractured reservoirs, different wells may exhibit significantly various production rates. Fracture cluster linkage can be attributed to various reasons, such as the reactivation of natural fractures, drilling of horizontal wells, and the generation of hydraulic fractures.

To analyze 80 outcrop maps, the cluster-check algorithm must be executed thousands of times. Hence, the implementation of an efficient cluster-check algorithm becomes imperative. In this study, we use a fast Monte Carlo algorithm (Newman & Ziff, 2001) and make the calculation computationally feasible (Zhu et al., 2022). The optimized cluster-check algorithm is 100 times more efficient than a highly cited open-source software, ADFNE (Alghalandis, 2017). In 80 outcrop maps collected, 63 shows spanning cluster, indicating good geometrical connectivity (Zhu, He, Santoso, et al., 2022). Six outcrop maps with different scales are selected as representatives to better illustrate results in the following section, while the full results for all outcrops are available in the Supporting Information (SI).

3. Results and Discussion

3.1. Impact of Fracture Sealing

In reality, inevitable fracture sealing degrades well-connected fracture networks into disconnected fracture clusters. The sealing patterns of natural fracture networks can be extremely complex, depending on the chemistry

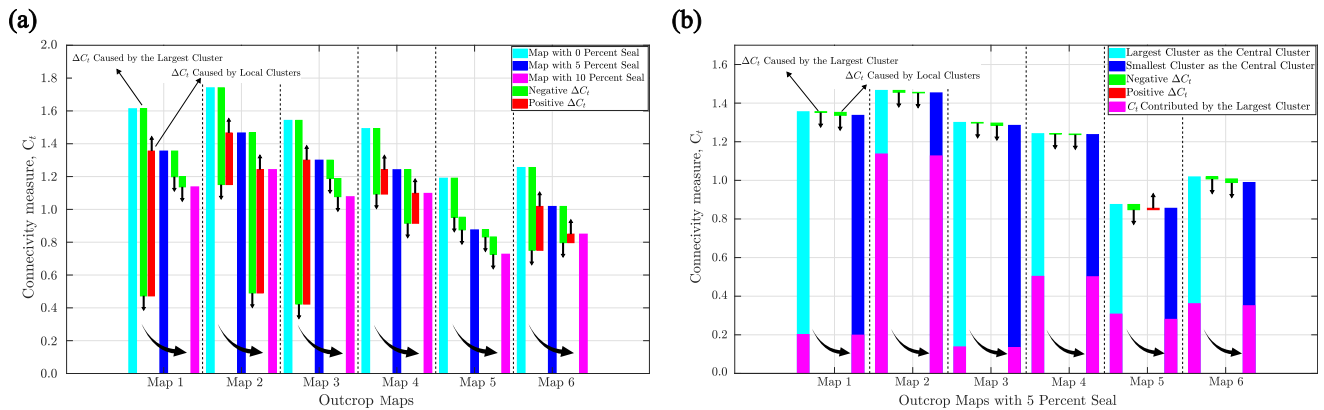


Figure 2. Connectivity variations for six outcrop maps considering (a) different degrees of fracture sealing and (b) central cluster alteration from the largest cluster (cyan bar) to the smallest cluster (blue bar). In panel (a), the cyan, blue, and magenta bars refer to the connectivity values of outcrop maps with 0, 5, and 10 percent of fracture sealing. The two green or red rectangles between two bars represent the connectivity variations caused by the changes in the largest cluster or local clusters.

of formation fluids, fluid pressure, and temperature (Laubach et al., 2004; Ukar & Laubach, 2016). To mimic sealing patterns and conduct a preliminary investigation into their impact, fractures are divided into small segments, and different proportions (5% and 10%) of fractures are randomly sealed. In the SI, a relatively realistic scenario is considered where a longer fracture has a lower probability of being sealed since it usually has a larger aperture, and vice versa. More complex sealing patterns, such as thin rinds or veneers, and bridge structures, are possible for implementation with given geostatistical rules. Fracture sealing also highly depends on fracture strength and current stress states. Critically stressed fractures can slip and enhance permeability (C. A. Barton et al., 1995). The stress-dependent sealing patterns can be further investigated with more knowledge of the fracture strength distribution, in situ stress states, and the failure criterion. For connectivity analysis, the sealed fracture segments are considered to have low permeability similar to the matrix. The largest cluster is chosen as the central cluster. The variations in connectivity considering different degrees of fracture sealing are shown in Figure 2a.

The more severe fracture sealing leads to lower connectivity of the fracture networks. From the original fracture map to the map with 5% sealing, the largest relative decrease is 26.5% in Map 5, and the least decrease is 15.7% in Map 3. The average decrease is 18.3% for the six chosen maps. From the fracture map with 5% fracture sealing to maps with 10% sealing, the largest decrease is 17.1% in Map 3, and the least decrease is 11.6% in Map 4. The mean decrease is 15.6% for the six selected maps.

For the entire collection of outcrop maps, the results are shown in (Figure S1 in Supporting Information S1). The mean decrease from the original maps to maps with 5% sealing is 19.1%, and from maps with 5% sealing to maps with 10% sealing, the mean decrease is 18.4%. For the relatively realistic scenario (Figure S2 in Supporting Information S1), similar results are obtained with a slightly more severe decrease in connectivity observed with fracture sealing. This is mainly because more short fractures are sealed, creating more local clusters. Therefore, fracture sealing has a significant impact on the entire fracture connectivity, with 5% of fracture sealing approximately decreasing 20% of the connectivity. Previous work concluded that a small proportion of fracture sealing can prevent the formation of spanning clusters in geometrically well-connected fracture networks (Zhu et al., 2022). With the newly defined connectivity metric, quantitative evaluation becomes possible.

Connectivity in fracture networks demonstrates a positive correlation with flow-related outcomes, such as permeability or production rate of the fractured formation, as shown in Figure 4. A water-gas flow simulation in a discrete fracture matrix system is conducted with UNCONG (Li et al., 2015). Detailed settings of the simulation, such as the relative permeability curve in the matrix and fractures, and boundary conditions, are consistent with previous work (Zhu, He, Li, et al., 2022). The fracture permeability is five orders of magnitude larger than that of the matrix to mimic a low-permeable formation. The pressure distributions in cases with different degrees of fracture sealing are illustrated in Figures 4a–4c. For the central cluster connected to the production well, gas easily transports to the fracture from the neighboring matrix and flows to the production well. In contrast, for local fracture clusters, the significant resistance in the matrix prevents efficient flow to the production well, resulting in

high pore pressure. The production performance sharply decreases with increasing sealing degree, as shown in Figure 4f.

A decrease in connectivity can be further decomposed into two factors: the first one is variation of connectivity attributed to the largest cluster, and the second is attributed to the remaining local clusters (see Figure 2a). Fracture sealing divides the original largest cluster into smaller clusters, thereby reducing the individual terms in Equation 1. Changes of the structure of a fracture network can have either a positive or negative impact on the interaction term in Equation 1. For the largest cluster, we observed that, across all 80 fracture maps, the individual term consistently outweighs the interaction term. Consequently, the first factor is always negative, leading to a reduction in connectivity. Regarding the remaining local clusters, fracture sealing increases the number of local clusters but decreases the size of each cluster. Therefore, the impact of fracture sealing on the individual term can be either positive or negative. Combining this term with an uncertain interaction term, results in either a negative or positive effect on connectivity. The results in Figure 2a (Figures S3–S12 in Supporting Information S1) indicate that in most cases local clusters contribute to an increase in connectivity.

3.2. Impact of Central Cluster Alteration

The detailed structures of fracture networks in the subsurface are unknown in most cases. Therefore, in engineering practice, vertical wells may or may not intersect with fracture clusters. In fractured reservoirs, neighboring wells may exhibit significantly different production rates. The following analysis can partially explain such phenomena from a perspective of connectivity variations caused by different well locations.

Alteration of the central cluster, shifting from the largest to the smallest, represents the best and worst scenarios in an actual drilling process. The corresponding variations in connectivity are depicted in Figure 2b. To simulate a scenario closer to reality, we opt for 5% of fractures to be sealed. The original map without any fracture sealing, along with maps featuring 10% fracture sealing, are available in (Figures S13–S15 and Tables S2–S4 in Supporting Information S1). The results indicate that the decrease in connectivity is marginal, and the impact of central clusters is insignificant. These minor variations primarily result from the standardization of the coefficients (relative permeability and viscosity of the interaction term) and the shortest distance calculation, where only distances with high resistance in the matrix are considered. Fractures exhibit significantly higher permeability than the matrix; thus, their resistance is negligible compared to that of the matrix. The distance through fracture clusters is excluded, rendering the impact on the interaction terms of connectivity negligible.

According to the decomposition results, ΔC_i caused by the largest cluster consistently exhibits a negative trend, as expected. ΔC_i caused by local clusters can be either negative or positive, but it is more likely to be negative (also as observed in Figures S16–S25 in Supporting Information S1). Since the numbers and relative sizes of clusters remain unchanged, the decrease is attributed to the diminished interaction term for both the largest cluster and local clusters.

In the original map, altering the central cluster results in a mean decrease of 1.1% across six selected outcrop maps. With 5% sealing, the mean decrease reaches 1.5%, and with 10% fracture sealing, it further rises to 2.1%. Comparing the original maps to those with varying degrees of sealing, there is a consistent upward trend in the mean decrease of connectivity. If this trend persists, altering clusters may have a notable impact on overall connectivity. Actual fracture sealing can be significant, breaking down the well-connected fracture networks into poorly connected ones and reducing overall connectivity.

In the original fracture outcrop maps, the majority of fracture networks are well-connected, with 63 out of 80 forming a spanning cluster. Hence, the connectivity of the entire fracture network is typically dominated by the largest cluster. Changing central clusters has a minor impact on the interaction term for the largest cluster, resulting in a final reduction in connectivity that is insignificant compared to the cases with fracture sealing. In cases with fracture sealing, fracture clusters have more uniform sizes, and the entire network connectivity is not predominantly controlled by a single large cluster but by several local clusters. Consequently, changes in the central cluster have a more significant negative impact on connectivity.

Additionally, Figure 2b illustrates the connectivity contribution of the largest cluster in magenta. It reveals that the largest cluster significantly contributes to connectivity, while the smallest cluster (central cluster) has an almost negligible connectivity contribution. As observed from Figures 4c, 4d, and 4f), matrix permeability is crucial to flow. Although the connectivity results of Figures 4c and 4d are close, the corresponding flow performances are

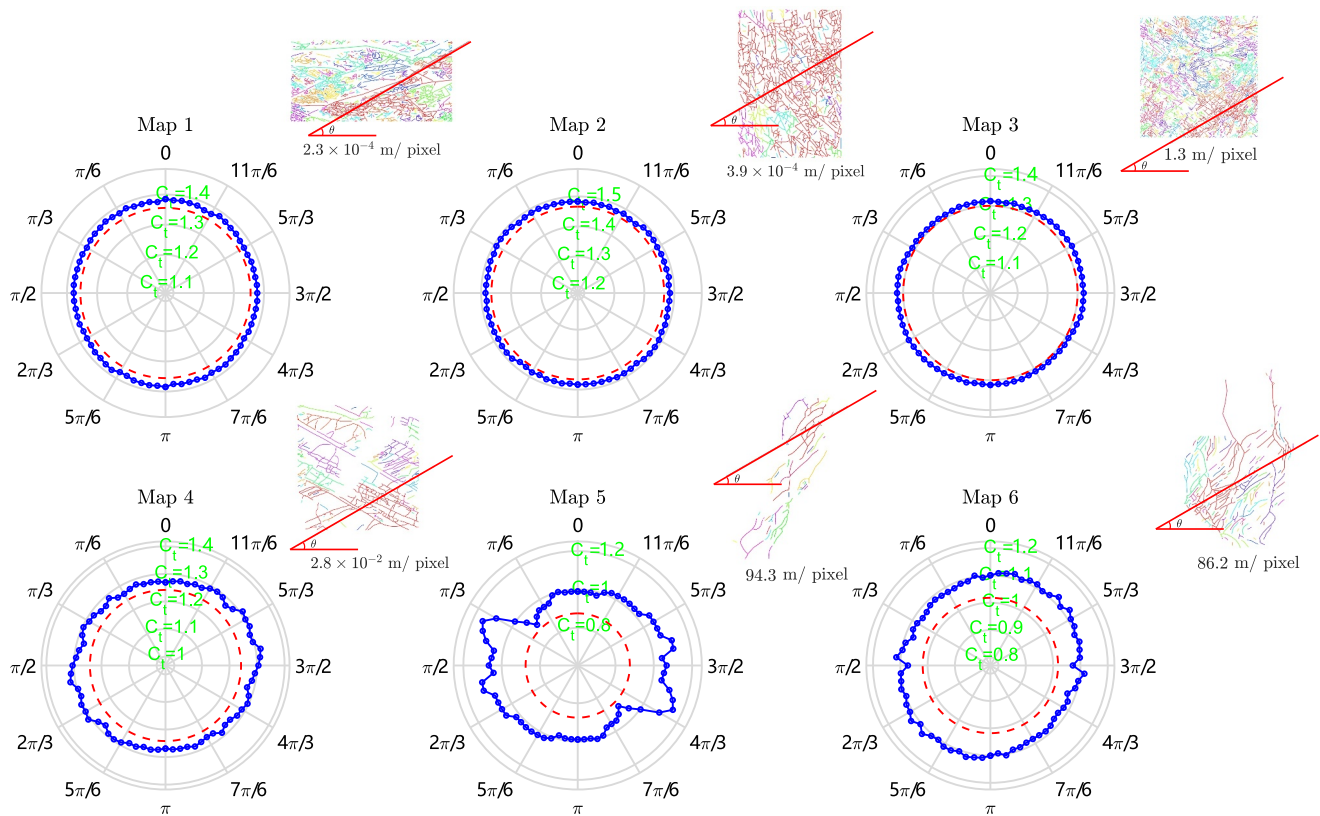


Figure 3. Connectivity variations for six outcrop maps in which individual clusters are linked by an infinitely long fracture with different orientations. To standardize the plot, we choose resolution (m/pixel) as the representative scale for the outcrop map.

significantly different. For the low-permeability formations, wells located in the largest cluster (Figure 4c) access more flow paths involving fractures, while wells intersecting the smallest cluster (Figure 4d) are isolated by a low-permeability matrix.

3.3. Impact of Cluster Linkage

To examine the impact of cluster linkage, we consider the addition of an infinitely long fracture centered at the centroid of the largest cluster within the system and connecting multiple clusters. Five percent of fractures are sealed to mimic reality. The orientation of the newly introduced fracture varies between 0 and π radians. The variations of connectivity resulting different fracture orientations are illustrated in Figure 3.

The addition of long fractures can enhance the connectivity of the fracture network by expanding the size of the largest clusters and simultaneously reduces the distance between local clusters and the central (largest) cluster. Maps 1, 2, and 3 have small variations in connectivity, while Maps 4, 5, and 6 exhibit a relatively large increase in connectivity, exceeding 5% for the maximum increase. From the outcrops shown in Figure 3, it is evident that Maps 1 to 3 have a more homogeneous distribution of fractures, while Maps 4 to 6 display a more heterogeneous and anisotropic pattern.

For heterogeneous and anisotropic cases, there exists an optimal orientation that can significantly increase the connectivity of the system. Map 5 achieves the highest connectivity increase (31.5%) at the orientation of $13/36 \pi$, and multiple clusters can be connected by the added long fracture. The complete results are available in (Figures S26–S38 and Table S5 in Supporting Information S1). Several outcrop maps that have fewer fractures and anisotropic distributions experience increases of more than 100%, with Map 58 showing the highest relative increase at 4,806%. Therefore, cluster linkage can always increase the connectivity of the fracture system, and heterogeneity and anisotropy plays a vital role.

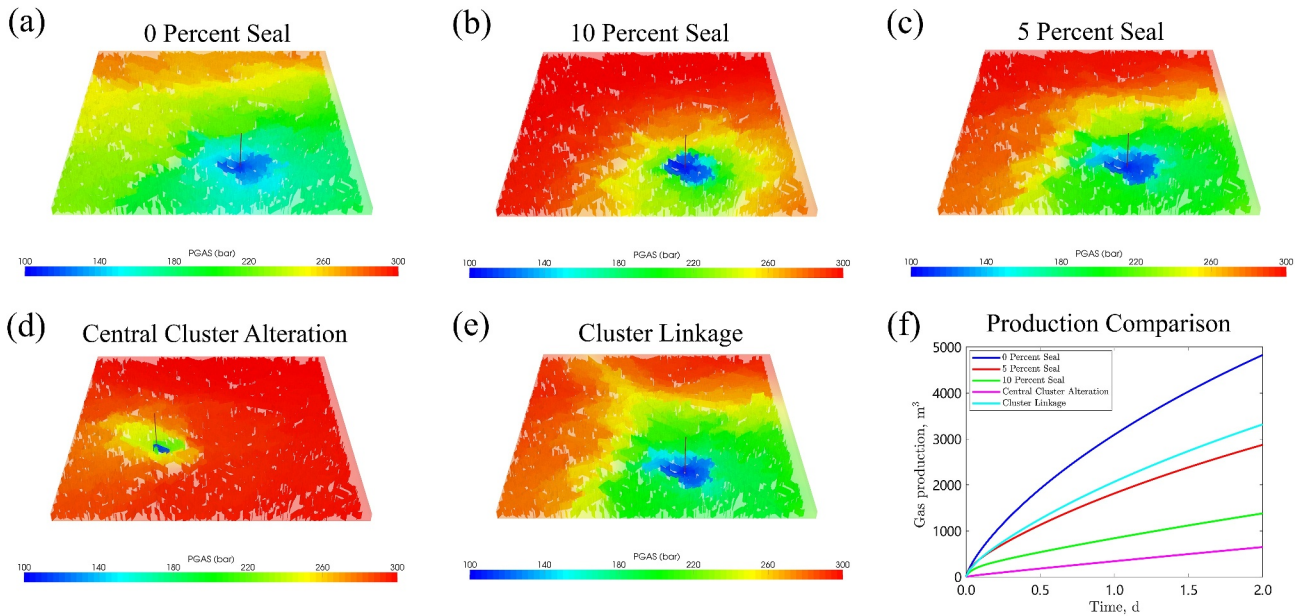


Figure 4. Gas pressure distribution in a water-gas flow simulation for different cases. The surface is intentionally made transparent to show the discrete fractures (Map 3).

Enhanced connectivity generally corresponds to higher hydraulic diffusivity and increased production rates. Therefore, linking multiple clusters at the optimal orientation through artificial treatment can substantially enhance production performance as observed in Figures 4e and 4f. In engineering applications, such as hydraulic fracturing, achieving the interconnection of multiple clusters is complex and depends on in-situ stresses, injected fluid properties, and treatment modes. Geostress determines orientation of horizontal wells and direction of hydraulic fractures, but natural fracture clusters also play a role in forming the stimulated reservoir volume and influence production (Zhu, He, Li, et al., 2022). The in-depth investigation of fracture initiation/reactivation and propagation is out of the scope of this work and will be addressed in future research. However, the formed fracture network is always a multi-cluster system due to the complex stress alteration and heterogeneity of rock strengths. Therefore, the proposed connectivity metric serves as a powerful tool for quantifying the evolving hydraulic fracture networks and can aid in well design.

3.4. Discussion

In this study, we expand the analysis from individual clusters to intricate systems comprising multiple clusters and enable the quantification of connectivity. The proposed connectivity metric can further include detailed fracture geometries, such as aperture and tortuosity of flow path within fractures. More complex connectivity metrics, such as global efficiency (Zhu et al., 2021), can be utilized to describe the connectivity of individual clusters in Equation 1. In addition, it is possible to combine pore network models and enhance the characterization of the connectivity in a more detailed fracture-matrix system. This quantification facilitates the exploration of connectivity variations within fracture networks and provides crucial insights for subsurface fluid transportation processes. Through the aforementioned analysis, it becomes feasible to optimize well placement and design strategies to interconnect multiple fracture clusters, consequently, enhancing overall network connectivity and improving well performances.

The connectivity index introduced in this research relies on the selection of a central cluster. We keep the central cluster choice in the connectivity calculation to describes its impact on the entire network connectivity. However, calculating an average over all clusters eliminates dependence on the selection of the central cluster, ensuring a more robust and unbiased evaluation of network connectivity.

$$C_i = \frac{1}{n} \sum_{j=0}^n \sum_{i=0}^n \left(\frac{k_m \mu_w}{k_f \mu} \right) \left(1 - \frac{d_{ij}}{d_{\max}} \right) \times \left(\frac{l_i}{l_{\text{total}}} \right) c_i \quad (4)$$

where d_{ij} is the shortest distance between the cluster i and cluster j . By adopting this approach, we transform the connectivity index into an independent parameter, directly associated with the structural rock characteristics and fluid properties.

The proposed metric is suitable for characterizing connectivity of complex fracture networks in 2D. However, actual fractures in the deep subsurface are always three-dimensional. The metric defined in Equation 1 can be conveniently extended to 3D fracture networks with slight adjustments.

$$C_t = \sum_{i=0}^n \underbrace{\left(\frac{k_m \mu_w}{k_f \mu} \right) \left(1 - \frac{d_i}{d_{\max}} \right)}_{\text{Interaction term}} \times \underbrace{\left(\frac{A_i}{A_{\text{total}}} \right)}_{\text{Individual term}} C_i \quad (5)$$

where d_i represents the shortest distance in the matrix from 3D cluster i to the central cluster; d_{\max} is the diagonal length of the bounding box that encloses all 3D fractures in the considered fracture system; A_i denotes the total area of fractures in cluster i ; A_{total} is the total area of all fractures in the system; and C_i is the connectivity metric of 3D cluster i . To calculate d_i , similar procedures in 2D cases are implemented. The only difference is to calculate the shortest distance between two neighboring clusters i and j . If the 3D fracture is represented by polygons, the shortest distance between neighboring clusters is determined by finding the shortest distance between all pairs of polygons in the i th fracture cluster and the j th cluster. This problem is further decomposed into calculating the shortest distance between two polygons, which can be broken down into the shortest distance between the vertices and the polygon. Detailed information about 3D fracture networks in the deep subsurface is often inaccessible with current techniques, such as seismic maps or wellbore images. Consequently, this limitation hinders the implementation of the metric to evaluate connectivity in actual subsurface fracture networks and provide optimization strategies to enhance well performance. Additionally, factors like well size, density, and trajectory are crucial for evaluating interactions between natural structures and artificial equipment. Stochastic Discrete Fracture Networks (SDFN) offer a practical alternative for generating complex fracture networks in 2D, 3D, and 4D (accounting for the fracture growth process) (Zhu et al., 2022). Through Monte Carlo or Latin hypercube sampling methods, it is feasible to generate thousands of realizations of complex 3D fracture networks considering various geometric patterns. Subsequently, systematic analysis of their connectivity evolution becomes possible. The novel connectivity metric proposed in this work serves as a fundamental tool. When combined with the powerful capabilities of HATCHFRAC (Zhu et al., 2022), an in-house discrete fracture network software, more in-depth investigations can help us better understand the complex nature of subsurface formations.

4. Conclusions

In this work, we proposed a new metric to quantify the connectivity of complex fracture networks composed of multiple clusters. By investigating the connectivity variations considering fracture sealing, alteration of central clusters, and cluster linkage, several important conclusions can be summarized as below:

- Fracture sealing strongly impacts overall fracture connectivity, with 5 percent of sealed fractures reducing connectivity by approximately 20 percent.
- The connectivity reduction is small when transitioning the central cluster from the largest to the smallest one. However, the largest cluster significantly contributes to overall connectivity, and the smallest one contributes minimally, which can partially explain the divergent well production performances in the same fractured formation.
- Natural fracture networks increase connectivity by linking more clusters, with heterogeneity and anisotropy playing a pivotal role in governing this increase. For heterogeneous and anisotropic fracture networks, an optimal well orientation exists and can cause substantial enhancements in connectivity. These findings help to refine well drilling operations and optimize production performance.

Data Availability Statement

All the synthetically generated data used for connectivity analysis in the study are available at Mendeley Data via (Zhu, 2024) with a CC BY 4.0 license. The interpreted data for 80 outcrop maps are available at 4TU. ResearchData via (Zhu, 2021) with a CC0 license.

Acknowledgments

This project was supported by the Second Tibetan Plateau Scientific Expedition and Research Program (No. 2019QZKK0904), the National Key Research and Development Program of China (No. 2019YFA0708704), the Key Research Program of the Institute of Geology and Geophysics, CAS (No. IGGCAS-202201), and the National Natural Science Foundation of China (No. 4182501). The authors want to thank Dr. Xiang Li from Ennosoft and Prof. Dongxiao Zhang from the Eastern Institute of Technology for providing the UNCONG simulator to simulate two-phase flow in complex fracture-matrix systems (Li et al., 2015).

References

Alghalandis, Y. F. (2017). ADFNE: Open source software for discrete fracture network engineering, two and three dimensional applications. *Computers & Geosciences*, 102, 1–11. <https://doi.org/10.1016/j.cageo.2017.02.002>

Alghalandis, Y. F., Dowd, P. A., & Xu, C. (2015). Connectivity field: A measure for characterising fracture networks. *Mathematical Geosciences*, 47(1), 63–83. <https://doi.org/10.1007/s11004-014-9520-7>

Allard, D., & Group, H. (1993). *On the connectivity of two random set models: The truncated Gaussian and the Boolean*. In *Geostatistics tróia '92* (Vol. 1, pp. 467–478). Springer.

Barton, C. A., Zoback, M. D., & Moos, D. (1995). Fluid flow along potentially active faults in crystalline rock. *Geology*, 23(8), 683–686. [https://doi.org/10.1130/0091-7613\(1995\)023<0683:ffapaf>2.3.co;2](https://doi.org/10.1130/0091-7613(1995)023<0683:ffapaf>2.3.co;2)

Barton, C. C. (1995). *Fractals in the earth sciences*. Springer.

Barton, C. C., Hsieh, P. A., Angelier, J., Bergerat, F., Bourou, C., Dettinger, M., et al. (1989). *Physical and hydrologic-flow properties of fractures: Las Vegas, Nevada-Zion canyon, Utah-grand canyon, Arizona-yucca Mountain, Nevada, July 20-24, 1989*. Wiley Online Library.

Becker, I., Koehrer, B., Waldvogel, M., Jelinek, W., & Hilgers, C. (2018). Comparing fracture statistics from outcrop and reservoir data using conventional manual and t-Lidar derived scanlines in ca2 carbonates from the Southern Permian basin, Germany. *Marine and Petroleum Geology*, 95, 228–245. <https://doi.org/10.1016/j.marpetgeo.2018.04.021>

Berkowitz, B., Bour, O., Davy, P., & Odling, N. (2000). Scaling of fracture connectivity in geological formations. *Geophysical Research Letters*, 27(14), 2061–2064. <https://doi.org/10.1029/1999gl011241>

Bertrand, L., Géraud, Y., Le Garzic, E., Place, J., Diraison, M., Walter, B., & Haffen, S. (2015). A multiscale analysis of a fracture pattern in granite: A case study of the tamariu granite, catalunya, Spain. *Journal of Structural Geology*, 78, 52–66. <https://doi.org/10.1016/j.jsg.2015.05.013>

Bisdom, K. (n.d.). Burial-related fracturing in sub-horizontal and folded reservoirs: Geometry, geomechanics and impact on permeability.

Blum, J., Chadwell, C., Driscoll, N., & Zumberge, M. (2010). Assessing slope stability in the Santa Barbara basin, California, using seafloor geodesy and chirp seismic data. *Geophysical Research Letters*, 37(13). <https://doi.org/10.1029/2010gl043293>

Bond, C. E., Wightman, R., & Ringrose, P. S. (2013). The influence of fracture anisotropy on CO₂ flow. *Geophysical Research Letters*, 40(7), 1284–1289. <https://doi.org/10.1002/grl.50313>

Bour, O., & Davy, P. (1997). Connectivity of random fault networks following a power law fault length distribution. *Water Resources Research*, 33(7), 1567–1583. <https://doi.org/10.1029/96wr00433>

Bour, O., & Davy, P. (1998). On the connectivity of three-dimensional fault networks. *Water Resources Research*, 34(10), 2611–2622. <https://doi.org/10.1029/98wr01861>

Cormen, T. H., Leiserson, C. E., Rivest, R. L., & Stein, C. (2022). *Introduction to algorithms*. MIT press.

Duffy, O. B., Nixon, C. W., Bell, R. E., Jackson, C. A.-L., Gawthorpe, R. L., Sanderson, D. J., & Whipp, P. S. (2017). The topology of evolving rift fault networks: Single-phase vs multi-phase rifts. *Journal of Structural Geology*, 96, 192–202. <https://doi.org/10.1016/j.jsg.2017.02.001>

Galloway, E., Hauck, T., Corlett, H., Pană, D., & Schultz, R. (2018). Faults and associated karst collapse suggest conduits for fluid flow that influence hydraulic fracturing-induced seismicity. *Proceedings of the National Academy of Sciences*, 115(43), E10003–E10012. <https://doi.org/10.1073/pnas.1807549115>

Gillespie, P., Howard, C., Walsh, J., & Watterson, J. (1993). Measurement and characterisation of spatial distributions of fractures. *Tectonophysics*, 226(1–4), 113–141. [https://doi.org/10.1016/0040-1951\(93\)90114-y](https://doi.org/10.1016/0040-1951(93)90114-y)

Healy, D., Rizzo, R. E., Cornwell, D. G., Farrell, N. J., Watkins, H., Timms, N. E., et al. (2017). Fracpaq: A matlab[™] toolbox for the quantification of fracture patterns. *Journal of Structural Geology*, 95, 1–16. <https://doi.org/10.1016/j.jsg.2016.12.003>

Holland, M., Saxena, N., & Urai, J. L. (2009). Evolution of fractures in a highly dynamic thermal, hydraulic, and mechanical system-(ii) remote sensing fracture analysis, jabal shams, Oman mountains. *GeoArabia*, 14(3), 163–194. <https://doi.org/10.2113/geoarabia1403163>

Im, K., Elsworth, D., & Fang, Y. (2018). The influence of pre-slip sealing on the permeability evolution of fractures and faults. *Geophysical Research Letters*, 45(1), 166–175. <https://doi.org/10.1002/2017gl076216>

Jafari, A. (2011). *Permeability estimation of fracture networks (Unpublished doctoral dissertation)*. University of Alberta.

Laubach, S., Reed, R., Olson, J., Lander, R., & Bonnell, L. (2004). Coevolution of crack-seal texture and fracture porosity in sedimentary rocks: Cathodoluminescence observations of regional fractures. *Journal of Structural Geology*, 26(5), 967–982. <https://doi.org/10.1016/j.jsg.2003.08.019>

Li, X., Zhang, D., & Li, S. (2015). A multi-continuum multiple flow mechanism simulator for unconventional oil and gas recovery. *Journal of Natural Gas Science and Engineering*, 26, 652–669. <https://doi.org/10.1016/j.jngse.2015.07.005>

Matthäi, S. K., & Belayneh, M. (2004). Fluid flow partitioning between fractures and a permeable rock matrix. *Geophysical Research Letters*, 31(7). <https://doi.org/10.1029/2003gl019027>

Newman, M. E., & Ziff, R. M. (2001). Fast Monte Carlo algorithm for site or bond percolation. *Physical Review E*, 64(1), 016706. <https://doi.org/10.1103/physreve.64.016706>

Odling, N., Gillespie, P., Bourguin, B., Castaing, C., Chiles, J., Christensen, N., et al. (1999). Variations in fracture system geometry and their implications for fluid flow in fractures hydrocarbon reservoirs. *Petroleum Geoscience*, 5(4), 373–384. <https://doi.org/10.1144/petgeo.5.4.373>

Odling, N. E. (1997). Scaling and connectivity of joint systems in sandstones from western Norway. *Journal of Structural Geology*, 19(10), 1257–1271. [https://doi.org/10.1016/s0191-8141\(97\)00041-2](https://doi.org/10.1016/s0191-8141(97)00041-2)

Orellana, L. F., Giorgetti, C., & Violay, M. (2019). Contrasting mechanical and hydraulic properties of wet and dry fault zones in a proposed shale-hosted nuclear waste repository. *Geophysical Research Letters*, 46(3), 1357–1366. <https://doi.org/10.1029/2018gl080384>

Prabhakaran, R., Boersma, Q., Bezerra, F. F., & Bertotti, G. G. (2019). Fracture network patterns from the Brejões outcrop, Irecê Basin, Brazil (version 1) [Dataset]. *4TU.ResearchData*. <https://doi.org/10.4121/uuid:67cde05c-9e99-4cc4-8ccc-9f2666457d1f>

Prabhakaran, R., Urai, J. L., Bertotti, G., Weismüller, C., & Smeulders, D. M. (2021). Large-scale natural fracture network patterns: Insights from automated mapping in the lilstock (Bristol channel) limestone outcrops. *Journal of Structural Geology*, 150, 104405. <https://doi.org/10.1016/j.jsg.2021.104405>

Qi, S., Wu, F., Yan, F., & Lan, H. (2004). Mechanism of deep cracks in the left bank slope of jinping first stage hydropower station. *Engineering Geology*, 73(1–2), 129–144. <https://doi.org/10.1016/j.enggeo.2003.12.005>

Renard, F., McBeck, J., Kandula, N., Cordonnier, B., Meakin, P., & Ben-Zion, Y. (2019). Volumetric and shear processes in crystalline rock approaching faulting. *Proceedings of the National Academy of Sciences*, 116(33), 16234–16239. <https://doi.org/10.1073/pnas.1902994116>

Renard, P., & Allard, D. (2013). Connectivity metrics for subsurface flow and transport. *Advances in Water Resources*, 51, 168–196. <https://doi.org/10.1016/j.advwatres.2011.12.001>

- Renshaw, C. E., Schulson, E. M., & Sigward, S. J. (2017). Experimental observation of the onset of fracture percolation in columnar ice. *Geophysical Research Letters*, *44*(4), 1795–1802. <https://doi.org/10.1002/2016gl071919>
- Robinson, P. (1983). Connectivity of fracture systems—a percolation theory approach. *Journal of Physics A: Mathematical and General*, *16*(3), 605–614. <https://doi.org/10.1088/0305-4470/16/3/020>
- Sanderson, D. J., & Nixon, C. W. (2015). The use of topology in fracture network characterization. *Journal of Structural Geology*, *72*, 55–66. <https://doi.org/10.1016/j.jsg.2015.01.005>
- Segall, P., & Pollard, D. D. (1983). Nucleation and growth of strike slip faults in granite. *Journal of Geophysical Research*, *88*(B1), 555–568. <https://doi.org/10.1029/jb088ib01p00555>
- Thiele, S. T., Grose, L., Samsu, A., Micklethwaite, S., Vollgger, S. A., & Cruden, A. R. (2017). Rapid, semi-automatic fracture and contact mapping for point clouds, images and geophysical data. *Solid Earth*, *8*(6), 1241–1253. <https://doi.org/10.5194/se-8-1241-2017>
- Ukar, E., & Laubach, S. E. (2016). Syn- and postkinematic cement textures in fractured carbonate rocks: Insights from advanced cathodoluminescence imaging. *Tectonophysics*, *690*, 190–205. <https://doi.org/10.1016/j.tecto.2016.05.001>
- Watkins, H., Bond, C. E., Healy, D., & Butler, R. W. (2015). Appraisal of fracture sampling methods and a new workflow to characterise heterogeneous fracture networks at outcrop. *Journal of Structural Geology*, *72*, 67–82. <https://doi.org/10.1016/j.jsg.2015.02.001>
- Wyller, F. A. (2019). *Spatio-temporal development of a joint network and its properties: A case study from lilstock, UK (unpublished master's thesis)*. The University of Bergen.
- Xu, C., Dowd, P., Mardia, K., & Fowell, R. (2006). A connectivity index for discrete fracture networks. *Mathematical Geology*, *38*(5), 611–634. <https://doi.org/10.1007/s11004-006-9029-9>
- Ye, Z., Fan, X., Zhang, J., Sheng, J., Chen, Y., Fan, Q., & Qin, H. (2021). Evaluation of connectivity characteristics on the permeability of two-dimensional fracture networks using geological entropy. *Water Resources Research*, *57*(10), e2020WR029289. <https://doi.org/10.1029/2020wr029289>
- Zhu, W. (2021). Supplementary data to the article: Enhancing fracture network characterization: A data-driven, outcrop-based analysis (version 2) [Dataset]. *4TU.ResearchData*. <https://doi.org/10.4121/14865096.v2>
- Zhu, W. (2024). Supplementary data to the article: A novel connectivity metric of identified multi-cluster fracture networks in permeable formations (version 1) [Dataset]. *Mendeley Data*. <https://doi.org/10.17632/c73y5j36g2.1>
- Zhu, W., He, X., Khirevich, S., & Patzek, T. W. (2022). Fracture sealing and its impact on the percolation of subsurface fracture networks. *Journal of Petroleum Science and Engineering*, *218*, 111023. <https://doi.org/10.1016/j.petrol.2022.111023>
- Zhu, W., He, X., Li, Y., Lei, G., Santoso, R., & Wang, M. (2022). Impacts of fracture properties on the formation and development of stimulated reservoir volume: A global sensitivity analysis. *Journal of Petroleum Science and Engineering*, *217*, 110852. <https://doi.org/10.1016/j.petrol.2022.110852>
- Zhu, W., He, X., Santoso, R. K., Lei, G., Patzek, T. W., & Wang, M. (2022). Enhancing fracture network characterization: A data-driven, outcrop-based analysis. *Computers and Geotechnics*, *152*, 104997. <https://doi.org/10.1016/j.compgeo.2022.104997>
- Zhu, W., Khirevich, S., & Patzek, T. W. (2021). Impact of fracture geometry and topology on the connectivity and flow properties of stochastic fracture networks. *Water Resources Research*, *57*(7), e2020WR028652. <https://doi.org/10.1029/2020wr028652>
- Zhu, W., Khirevich, S., & Patzek, T. W. (2022). HatchFrac: A fast open-source DFN modeling software. *Computers and Geotechnics*, *150*, 104917. <https://doi.org/10.1016/j.compgeo.2022.104917>
- Zoback, M., & Smit, D. (2023). Meeting the challenges of large-scale carbon storage and hydrogen production. *Proceedings of the National Academy of Sciences*, *120*(11), e2202397120. <https://doi.org/10.1073/pnas.2202397120>